Journal of Thermal Analysis, Vol. 14 (1978) 253–264

THERMAL DECOMPOSITION OF POTASSIUM HEXACYANOFERRATE(II) TRIHYDRATE

J. I. KUNRATH, C. S. MÜLLER and E. FRANK

Instituto de Fisica, Universidade Federal do Rio Grande do Sul, Porto Alegre, Brasil

(Received August 28, 1977)

Potassium hexacyanoferrate(II) trihydrate, $K_4Fe(CN)_6 \cdot 3H_2O$, was heated under controlled conditions of mass and rate in a derivatograph in the presence of oxygen. The heating was stopped at different temperatures and Mössbauer spectra and X-ray diffractograms were taken on the quenched material at room temperature. The reaction pathway was studied in this way and the advantages and drawbacks of each of the techniques are described. At different stages of the thermal process we were able to show the presence of $K_4Fe(CN)_6$, α-Fe_2O_3, Fe_3O_4, Fe_3C, Fe, FeO, $KFeO_2$, β-FeOOH, KOCN, K_2CO_3 and KCN.

The subject of the thermal decomposition of hexacyanoferrates has been widely discussed in the literature [1–7]. Chamberlain and Green [1] and Seifer [2] started the systematic study of several of these compounds, using differential thermal analysis and dynamic gas evolution, after a number of early papers which report studies under a huge variety of conditions (see literature contained in Ref. [1]). For potassium hexacyanoferrate(II) they found at 100° a strong endothermic peak due to loss of water, and at 588° a weak, very broad peak due to cyanogen evolution. Seifer et al. [3, 4] investigated a number of cyanoferrates(II) using thermal-, X-ray and chemical analysis and Mössbauer spectroscopy, and concluded that the decomposition temperature of the ion was related to the ionic potential of the associated cation. Furthermore, if the associated cations belong to the first transition series and have an odd number of *d* electrons, the temperature of the initial decomposition is lower. Decomposition schemes are classified by these authors as hydrolytic or non-hydrolytic, and divided into three stages: a) dehydration of the salt; b) breakdown of the anionic complex; and c) further breakdown of the decomposition products. The heat treatment was of a static nature for 2 hr close to the temperature which corresponds to each of these stages. Reaction mechanisms were proposed which include the formation of cementite and its decomposition into Fe. Gallagher and Prescott [5] made a detailed study of the thermal decompositions of $EuFe(CN)_6 \cdot 5H_2O$ and $NH_4EuFe(CN)_6 \cdot 4H_2O$, and found that the chain of intermediates is $(Fe(CN)_6^{3-}$ or $Fe(CN)^{4-})$, $Fe(CN)_2$, Fe_3C and Fe. The study was performed under vacuum and in a nitrogen atmosphere. Fanning et al. [6] discuss the thermal decompositions of $H_4Fe(CN)_6$ and $H_3Fe(CN)_6$ at constant temperature in nitrogen, oxygen

and hydrogen, and propose the steps for the formation of Prussian blue. Raj and Danon [7] discuss the thermal decompositions of several hexacyanoferrates(III) up to 650° using the Mössbauer effect, and find that the presence of water lowers the decomposition temperature and may cause the formation of Fe_2O_3 at higher temperature. In the case of anhydrous complexes the end-product is iron metal, while in the case of hydrated complexes the corresponding hydrated alkali metal ferrites are formed. A reaction scheme is proposed which includes the formation of $Fe(CN)_2$.

In this paper we report results of a combined thermogravimetry (TG), differential thermal analysis (DTA), differential thermogravimetry (DTG), ^{57}Fe Mössbauer effect (ME) and X-ray diffraction investigation in which, by using a relatively low heating rate, we were able to isolate the reaction pathway and to show the relative advantages of one or another technique.

Experimental

The thermal analysis measurements were made with a derivatograph [8] (MOM, Budapest) which performs simultaneous TG, DTG and DTA and measures the temperature T within the sample. The ME spectrometer was a constant acceleration type with linearity better than 0.2 per cent over 95 per cent of the triangular wave form [9]. The source was 10 mC of ^{57}Co in Cu (NENC) and the spectrometer was calibrated with sodium nitroprusside and natural iron. Isomer shifts are given relative to the former [10]. The spectra were fitted with a least squares computing program which provided positions, widths, intensities and areas (and their errors) for all the peaks. Figure 2 shows the most relevant spectra. The others are referred to in Table 1.

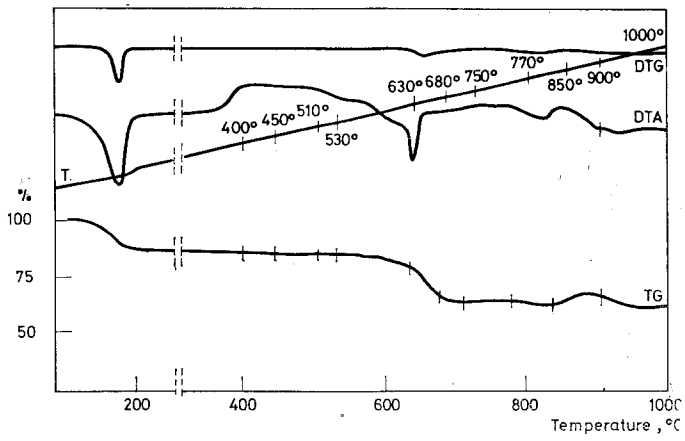

Fig. 1. Thermal analysis curves for the decomposition of 2000 mg of PFCNT at a rate of 2°/min

Table 1

Experimental results for Mössbauer spectra at room temperature of the decomposition products of 2000 mg of PFCN in air at a heating rate of 2°/min

Quenched from	δ, mm/s *vs.* Fe	ΔE_Q, mm/s	H_{eff}, kOe	Compound	%*
R. T.	0.02±0.03	0	0	$K_4Fe(CN)_6 \cdot 3H_2O$	100
150°	0.03±0.03	0	0	$K_4Fe(CN)_6$	100
400°	0.02±0.03	0	0	$K_4Fe(CN)_6$	100
450°	0.01±0.04	0	0	$K_4Fe(CN)_6$	47 (1)
	0.34±0.04	0.09±0.04	517±5	α-Fe_2O_3	53 (5)
480°	0.02±0.03	0	0	$K_4Fe(CN)_6$	31 (1)
	0.40±0.03	0.09±0.03	516±5	α-Fe_2O_3	69 (5)
	0.01±0.03	0	0	$K_4Fe(CN)_6$	19 (1)
510°	0.39±0.03	0.09±0.03	516±5	α-Fe_2O_3	51 (4)
	—	—	—	Fe_3O_4	30 (5)**
	0.03±0.03	0	0	$K_4Fe(CN)_6$	3 (1)
530°	0.28±0.03	0.05±0.03	487±4	Fe_3O_4(A)	43 (10)
	0.72±0.03	0.04±0.03	461±4	Fe_3O_4(B)	54 (10)
	0.28±0.03	0.04±0.03	486±4	Fe_3O_4(A)	44 (10)
580°	0.70±0.03	0.03±0.03	462±4	Fe_3O_4(B)	53 (10)
	0.03±0.03	0	0	$K_4Fe(CN)_6$	3 (1)
	—	—	485±4	Fe_3O_4(A)	
630°	—	—	461±4	Fe_3O_4(B)	39 (7)**
	0.25±0.03	0.00±0.03	210±3	Fe_3C	61 (5)
	0.25±0.03	0.00±0.03	208±3	Fe_3C	56 (3)
680°	0.01±0.03	0	0	$K_4Fe(CN)_6$	29 (2)
	—	—	330±3	Fe	15 (5)**
	0.22±0.03	0.00±0.03	209±3	Fe_3C	91 (3)
730°	0.01±0.03	0	0	$K_4Fe(CN)_6$	3 (3)
	—	—	328±3	Fe	6 (6)**
	0.05±0.03	0.01±0.03	331±3	Fe	68 (3)
770°	0.28±0.05	0.04±0.05	484±6	Fe_3O_4(A)	16 (5)
	0.70±0.05	0.03±0.05	461±6	Fe_3O_4(B)	16 (5)
	0.05±0.03	0.01±0.03	330±3	Fe	18 (6)
850°	0.37±0.03	0.03±0.03	490±4	Fe_3O_4(A)	15 (3)
	0.70±0.05	0.03±0.05	460±6	Fe_3O_4(B)	15 (6)
	1.01±0.03	0.69±0.03	0	FeO	52 (2)
	0.24±0.03	0.03±0.03	500±5	$KFeO_2$	80 (7)
900°	0.35±0.03	0.73±0.03	0	β-FeOOH	10 (1)
	—	—	460±6	Fe_3O_4	10 (8)**, +
1000°	0.21±0.03	0.04±0.03	500±5	$KFeO_2$	87 (3)
	0.35±0.03	0.70±0.03	0	β-FeOOH	13 (2)

* Referred to the total amount of iron detected by ME (estimated error of the reported values is given in brackets).

** Calculated as the balance amount.

\+ For sites *A* plus *B*.

Powder diffraction analysis of the samples was made on a Rigaku Denki Co. model 2011 B diffractometer, using CoK_α radiation selected with an iron filter.

Thermal analysis measurements were made using 2000 mg of reagent grade $K_4Fe(CN)_6 \cdot 3H_2O$ (PFCNT) in air in a Pt crucible at a rate of 2°/min (Fig. 1). All ME spectra shown were taken with specimens produced by quenching the

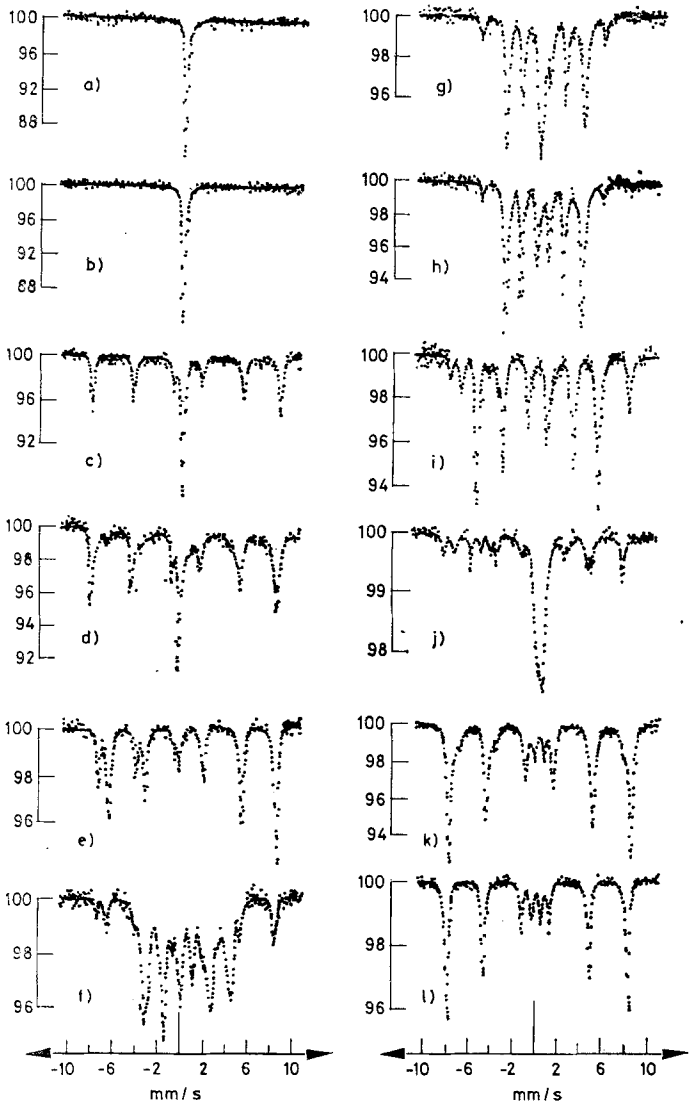

Fig. 2. Room temperature Mössbauer spectra of PFCNT (2000 mg) heated at a rate of 2°/min and quenched from: a) room temperature; b) 150°; c) 450°; d) 510°; e) 530°; f) 630°; g) 680°; h) 730°; i) 770°; j) 850°; k) 900°; l) 1000°

reaction crucible (directly from the derivatograph) in air from a given temperature down to room temperature. In this way the thermal history of a given specimen is known up to the quenching point. The actual ME and X-ray measurements were all made at room temperature and the sample encapsulation was made under argon. The hygroscopic nature of the products demands manipulation in a dry atmosphere.

Representativity of the samples used in the X-ray and ME determination was not always perfect, due either to loss of material or strong adherence to the crucible walls. Therefore, only a relative value must be ascribed to the reported concentrations of the different compounds within the samples.

Results and interpretation

Figure 1 gives the pattern of the thermal analysis parameters of PFCNT, using a 2000 mg sample. It shows at 150° an endothermic peak with a 13% weight loss, which corresponds to the loss of 3 molecules of water. The process starts at around 100°. X-ray diffraction confirms that anhydrous $K_4Fe(CN)_6$ (PFCN) has been formed (Table 2). ME spectra of both species show practically the same shift, in agreement with the data of the literature [11] (Table 1 and Fig. 2a, 2b).

Preliminary results show that the later stages of the thermal decomposition depend on the amount of material used.

The experiment with 2000 mg samples, after the dehydration stage, can be described under 3 headings: first oxidation, reduction and second oxidation, which we will describe in detail.

i) First oxidation

Thermal treatment up to 400° did not introduce any change in the sample, as shown by the ME and X-ray parameters (Tables 1 and 2). When the sample was heated up to 450° a drastic change occurred in the ME spectrum, as 7 lines were found (Fig. 2c). Computer fitting shows that around 47% of the iron still corresponds to PFCN, whereas the remaining ME absorption corresponds to the 6-line pattern of hematite (α-Fe_2O_3), as shown by the magnetic splitting, which was found to be 517 ± 5 kOe [12]. The diffraction pattern shows, in agreement, PFCN, α-Fe_2O_3 and KOCN [13] (Tables 1 and 2). This suggests that the PFCN in the upper part of the crucible, when attaining 450°, reacted with O_2 of the air. The following reactions are suggested:

$$4\ K_4Fe(CN)_6 + 3\ O_2 \rightarrow 2\ Fe_2O_3 + 16\ KCN + 4\ (CN)_2 \quad (1)$$

$$2\ KCN + O_2 \rightarrow 2\ KOCN \quad (2)$$

Cyanogen is gaseous and therefore lost from the system.

Table 2

Compounds detected through Mössbauer effect and X-ray analysis

Quenched from	Mössbauer effect	%*	X-ray
R. T.	$K_4Fe(CN)_6 \cdot 3H_2O$	100	$K_4Fe(CN)_6 \cdot 3H_2O$
150°	$K_4Fe(CN)_6$	100	$K_4Fe(CN)_6$
400°	$K_4Fe(CN)_6$	100	$K_4Fe(CN)_6$
450°	$K_4Fe(CN)_6$ α-Fe_2O_3	47 (1) 53 (5)	$K_4Fe(CN)_6$ α-Fe_2O_3 KOCN
510°	$K_4Fe(CN)_6$ α-Fe_2O_3 Fe_3O_4	19 (1) 51 (4) 30 (5)	$K_4Fe(CN)_6$ α-Fe_2O_3 Fe_3O_4 KOCN
580°	$K_4Fe(CN)_6$ Fe_3O_4	3 (1) 97 (10)	$K_4Fe(CN)_6$ Fe_3O_4 K_2CO_3 $K_4Fe(CN)_6$ Fe_3C K_2CO_3 KCN
680°	$K_4Fe(CN)_6$ Fe_3C Fe	29 (2) 56 (3) 15 (5)	$K_4Fe(CN)_6$ Fe_3C K_2CO_3 KCN
730°	$K_4Fe(CN)_6$ Fe_3C Fe	3 (3) 91 (3) 6 (6)	Fe_3C K_2CO_3
770°	Fe Fe_3O_4	68 (3) 32 (10)	Fe K_2CO_3
850°	Fe Fe_3O_4 FeO	18 (6) 30 (9) 52 (2)	
900°	$KFeO_2$ Fe_3O_4 β-FeOOH	80 (7) 10 (8) 10 (1)	
1000°	$KFeO_2$ β-FeOOH	87 (3) 13 (2)	$KFeO_2$ $K_2CO_3 \cdot 1 \cdot 5H_2O$

* Referred to the total amount of iron detected by M. E. (estimated error of the reported value in brackets).

Table 1 shows that the only difference between the spectra of the mixtures obtained at 450° and 480° is the ratio of the two compounds, which favours α-Fe_2O_3 with increasing temperature.

As mentioned above, Chamberlain and Greene [1] list the temperature of 588° for $(CN)_2$ evolution. As a matter of fact, they do not show a gas evolution curve and the DTA reveals only a very smooth change in the baseline, which does not allow a precise determination of the temperature. Nevertheless, the higher value found by these authors does not conflict with our results, as the reaction which produces $(CN)_2$ is different to the one we propose, due to the lack of O_2 in their system.

ii) Reduction

Spectra of the higher-temperature products show that from 510° upward there is a reduction of the amounts of hematite and of PFCN as shown in Fig. 2d and Tables 1 and 2. The resolution of this spectrum was not good enough to obtain the ME parameters of the newly-appearing compound, which was shown by X-ray diffraction to be Fe_3O_4.

The Mössbauer spectra of the 530° sample is much better resolved and displays the classical 12-line spectrum of magnetite due to the population of both sites of the inverse spinel [12], the tetrahedral and the octahedral ones, superimposed with a small contribution of PFCN (see Table 1 and Fig. 2e). The sample shows a total absence of hematite.

We suggest the following mechanism for the reduction of hematite to magnetite after the initial decomposition of the PFCN with loss of 1/3 of the cyanide radicals (Eqs. (1) and (2)). The first step corresponds to a degenerative cycle for the potassium cyanate

$$4\ KOCN \rightarrow K_2CO_3 + 2\ KCN + CO + N_2 \qquad (3)$$

whereas the second step corresponds to the reduction of Fe_2O_3 according to

$$3\ Fe_2O_3 + CO \rightarrow 2\ Fe_3O_4 + CO_2 \qquad (4)$$

Tables 1 and 2 summarize the data for the sample obtained at 580°. We must remark that the ME data were obtained with a sample taken from the upper part of the crucible, as there was a natural separation into two neat layers (shown in Table 2 with a heavy line), an upper black one and a lower grey one. The X-ray pattern of the former showed Fe_3O_4, PFCN and K_2CO_3, whereas that of the latter showed PFCN, K_2CO_3, Fe_3C and KCN. For safety reasons, this sample was immediately disposed of and ME measurements were not made.

The fact that Fe_3O_4 was found only in the upper part of the crucible explains he existence of anhydrous PFCN at 580°, as the oxide isolates the lower part trom contact with the air.

We recall that a similar process takes place in the industrial method of cyaniding for steel hardening where the reaction [14]

$$2\ CO + 3\ Fe \rightarrow Fe_3C + CO_2 \qquad (5)$$

takes place.

The following tentative explanation is not absolutely satisfactory. We suggest that the necessary metallic iron would appear as indicated by Moffett et al. [15] for the thermal decomposition of sodium hexacyanoferrate(II) in the absence of oxygen through the reaction

$$K_4Fe(CN)_6 \rightarrow 4\ KCN + Fe + N_2 + 2\ C \qquad (6)$$

This reaction is not in agreement with reference [1], probably due to the fact that several pathways are possible and the actual one depends on the employed conditions, which differ in the two cases. If reaction (6) really takes place in the lower part of the crucible and reaction (4) mainly in the upper part, it is difficult to explain the efficiency of reaction (5) in the present case. An alternative explanation, which does not present this weak point, involves reaction (6')

$$K_4Fe(CN)_6 \rightarrow 4\ KCN + Fe + (CN)_2 \qquad (6')$$

followed by the reaction of Fe with cyanogen

$$6\ Fe + (CN)_2 \rightarrow 2\ Fe_3C + N_2 \qquad (6'',)$$

Anyhow, we have no arguments which unambiguously confirm these reactions and many other pathways may be conceived.

At 580° these reactions are confined to the lower part of the crucible, but at around 630° the DTA curve shows a sharp drop due to the onset of the melting of KCN (m.p. = 634.5°); this compound obstructs the outflow of gases such as N_2, CO_2, etc. When the pressure is high enough, the liquid is forced outside the crucible and spilling occurs against the quartz bell. For this reason the loss indicated in the TG curve is not centered exactly on the transition temperature. The 630° sample ME spectrum shows an overlap of the magnetite and cementite spectra [12], with a ratio of nearly 2 to 3 (Table 1; Fig. 2f).

The 680° sample (Tables 1 and 2; Fig. 2g) shows a significant conversion to cementite. Neither the X-ray diffractogram nor the ME spectrum reveal any peaks due to Fe_3O_4, but the ME spectrum starts showing up neatly the first and sixth lines of iron. This compound does not appear in the diffractogram, which on the contrary shows clearly K_2CO_3 and KCN. Both the X-ray and the ME patterns reveal the existence of unreacted PFCN.

The 730° sample (Table 2) shows neither PFCN nor α-iron in the X-ray powder diffraction diagram, but cementite and KCN. On the other hand, the ME spectrum shows Fe_3C, together with a small proportion of α-iron and PFCN (Table 1, Fig. 2h). The existence of PFCN up to this temperature is due to a lack of diffusion of oxygen towards the lower part of the crucible. Summing up, at this step we

observe a quasi-complete transformation of the PFCN into Fe_3C and traces of α-iron plus K_2CO_3. The strong mass loss is due to volatization of CO_2 and N_2.

iii) Second oxidation

In the previous step we found a progressive formation of Fe_3C and the consequent decrease of metallic Fe. At 770° this tendency reverts. The rise from 6 to nearly 68 per cent of Fe (even if not absolutely reliable) is indicative of the trend. Fe_3C disappears completely, as shown in Tables 1 and 2 and Fig. 2i. This suggests that somewhat below this temperature the reaction

$$Fe_3C + O_2 \rightarrow 3\ Fe + CO_2 \qquad (7)$$

occurs. The lack of stability of cementite at high temperatures is a well-known fact, and of utmost relevance in the steel industry [14].

Part of the Fe oxidizes and forms magnetite

$$3\ Fe + 2\ O_2 \rightarrow Fe_3O_4 \qquad (8)$$

as shown by the ME spectrum of the 770° sample. The X-ray pattern shows α-iron plus K_2CO_3, but no traces of magnetite. A certain degree of discrepancy between the results of the two techniques could be explained as due to differences in sampling, but such a gross difference must be due to other – more fundamental – reasons, such as problems of poor crystallization of the magnetite, and the higher intrinsic ability of ME to detect the formation of compounds.

The overall explanation for this oxidative step seems to be a larger diffusion of oxygen into the crucible, due to thermal agitation.

Between 770 and 830° the TG curve shows a small weight loss, which reverts at this temperature in agreement with the inflection of the DTA curve, which indicates the beginning of an exothermic reaction with a maximum at nearly 850°. The ME spectrum of the product obtained when stopping the heating at 850° (Fig. 2j) exhibits similarities with the 770° sample (Fig. 2i), as all the lines of the latter are found in the former, but with a difference in intensities. In addition, a strong doublet (around 52% of the area), which does not exist in the former sample, appears. This spectrum can be considered as produced by wűstite (Fe_xO), in agreement with literature data. The slight asymmetry of the two peaks can be ascribed to the overlap of a doublet due to Fe^{2+} (or two, depending on the model) plus a singlet due to the Fe^{3+}, which arises from the structural defects due to cation vacancies. The separation of the two peaks can also be correlated with the "x" value of the wűstite [12]. A tentative explanation for the appearance of wűstite may be the following: at around 800° the dissociation pressure of K_2CO_2 is alredy significant (around 1 mm Hg), and together with whatever amount of CO_2 is still existing in the medium (and originating in the reaction described by equation (7)) reacts according to:

$$CO_2 + x\ Fe \rightarrow Fe_xO + CO \qquad (9)$$

A reaction which may occur simultaneously is

$$K_2CO_3 + x\,Fe \rightarrow K_2O + Fe_xO + CO \tag{10}$$

Magnetite disappearance could be explained by CO reduction:

$$x\,Fe_3O_4 + (4x - 3)\,CO \rightarrow 3\,Fe_xO + (4x - 3)\,CO_2 \tag{11}$$

The weight increase found at around 830° can be ascribed to the subsequent oxidation of wűstite:

$$2\,Fe_xO + \left(\frac{3}{2}x - 1\right)O_2 \rightarrow x\,Fe_2O_3 \tag{12}$$

but neither the ME data nor the X-ray diffraction pattern could confirm this, as the 900° sample (Table 1, Fig. 2k) shows a 6-peak pattern with a magnetic field of 500 ± 5 k Oe. This value can hardly be ascribed to α-Fe_2O_3, as the value found in the literature (518 kOe) [12] falls well outside our value taking into account both experimental errors. Two possibilities arise: we are dealing either with maghemite (γ-Fe_2O_3), with a hyperfine field of 505 ± 2 kOe at 300 K [12], or with potassium orthoferrite, for which the values 502 and 494 kOe have been reported [16, 17]. Superimposed on this we find a weak spectrum apparently due to Fe_3O_4, and a considerable amount of a paramagnetic compound which is suspected to be β-FeOOH [18], due perhaps to a partial rehydration. The X-ray powder pattern was of poor quality due to the extremely hygroscopic nature of the decomposition products, and added no further information. This was improved using a suitable transparent plastic sheet to cover the sample which was obtained at 1000° [19]. The X-ray powder diffraction diagram clearly showed the presence of potassium ferrite, $KFeO_2$ (Table 2). The ME spectrum displays qualitatively the same features as the one corresponding to the 900° sample, but with a negligible contribution of the lower-field compound found in the previous spectrum, Fe_3O_4 (Tables 1 and 2, Fig. 2). The reaction products of these samples left exposed to air have also been studied, but will be described elsewhere.

The formation of potassium ferrite, $KFeO_2$, can be explained through two reactions

$$Fe_2O_3 + K_2O \rightarrow 2\,KFeO_2 \tag{13}$$

or direct reaction of the oxide with the carbonate:

$$Fe_2O_3 + K_2CO_3 \rightarrow 2\,KFeO_2 + CO_2 \tag{13b}$$

Probably both reactions occur simultaneously. The second one agrees with the method proposed by Ichida et al. [16] for the synthesis of $KFeO_2$. The fact that Fe_2O_3 has not been found in these steps gives an indication of the speed of these reactions.

Final remarks

The joint use of thermal techniques, ME and X-ray diffraction, allowed us to study the thermal decomposition of $Fe(CN)_6K_4 \cdot 3H_2O$ in air from room temperature up to 1000°. Four well-differentiated stages have been found when using 2000 mg with a heating rate of 2°/minute: dehydration, oxidation, reduction and second oxidation. Preliminary studies show that the behaviour depends on the mass employed. The information obtained from each technique is in general of a complementary nature, as shown in Table 2 for X-ray and ME. X-ray diffraction analysis, usually accepted as the analytical method par excellence, proved sometimes to be neither easy nor quick, nor precise, and sometimes was even impossible. For example, the X-ray powder pattern of the product in the lower part of the crucible, obtained at 580°, showed 53 lines of more than 20% intensity. In this sense the limitations of ME as an identification technique, namely its isotope selectiveness, turn out to be very helpful in simplifying the complex spectra. In spite of this, in two instances (150 and 1000° samples) the identification had to rely on the X-ray measurements because of the inconclusiveness of the ME analysis.

On the other hand, the detection limit of ME is much less dependent on the particle size than for the X-ray diffraction pattern. This was the case with the 680° and 730° samples for Fe, and at 770° for Fe_3O_4. Further, small amounts of a compound sometimes show up more easily in Mössbauer spectra than in X-ray diffraction patterns, as with PFCN at 730°. Quantitative interpretation in the case of ME spectra is hampered by the fact that the hypothesis of equal f (Lamb–Mössbauer) factors has to be made, especially for samples containing several compounds. Therefore, the experimental values have to be taken only as indicative of the order of magnitude. For the X-ray diagrams the above-mentioned grain size factor and the absorption coefficients of the compounds are the main difficulties in the quantitative interpretation. Therefore, a judicious application of those techniques permits an adequate qualitative interpretation as shown above.

*

This research was performed with financial support from the Conselho Nacional de Desenvolvimento Científico e Tecnológico (CNPq) and Financiadora de Estudos e Projetos (FINEP). We are grateful to Profs. A. Bristoti, J. Danon, P. J. Aymonino, E. Baran and M. A. Blessa for valuable suggestions and criticisms, and Miss E. A. Veit for performing the thermal measurements at the Pontificia Universidade Católica, Porto Alegre. This work was submitted in partial fulfilment of the conditions for the degree of "Livre Docente" by one of us (J. I. K.).

References

1. M. M. CHAMBERLAIN and A. F. GREENE, J. Inorg. Nucl. Chem., 25 (1963) 1471.
2. G. B. SEIFER, (a) Zh. Neorg. Khim. 5 (1960) 68; (b) ibid. 7 (1962) 482.
3. G. B. SEIFER and Z. A. MAKAROVA, Dokl. Akad. Nauk. SSR, 169 (1966) 358.

4. B. V. BORSHAGOVSKII, V. I. GOLDANSKII', G. B. SEIFER and R. A. STUKAN, Russ. J. Inorg. Chem., 12 (1967) 1741.
5. P. K. GALLAGHER and B. PRESCOTT, Inorg. Chem., 9 (1970) 2510.
6. J. C. FANNING, C. D. ELROD, B. S. FRANKE and J. D. MELNIK, J. Inorg. Nucl. Chem. 34 (1972) 139.
7. D. RAJ and J. DANON, J. Inorg. Nucl. Chem., 37 (1975) 2039.
8. F. PAULIK, J. PAULIK and L. ERDEY, Talanta, 13 (1966) 1409.
9. M. I. DA COSTA JR., Thesis, Universidade Federal do Rio Grande do Sul, Porto Alegre, Brasil, 1976.
10. Nomenclature and Conventions for Reporting Mössbauer Spectroscopic Data, in Mössbauer Effect Data Index (covering the 1971 literature), J. G. Stevens and V. E. Stevens, eds. (Plenum Press N. Y.) 1972.
11. Y. HAZONY, J. Chem. Phys., 45 (1966) 266.
12. N. N. GREENWOOD and T. C. GIBB, Mössbauer Spectroscopy, Chapman & Hall, London 1971 (and literature therein contained).
13. Powder Diffraction File Search, published by the Joint Committee on Powder Diffraction Standards, Swarthmore, Penn., USA (1974).
14. V. CHIAVERINI, Aços carbono e aços ligas, Universidade de São Paulo, Brasil, 1955.
15. E. C. MOFFETT and J. JACKSON, Ferrocyanides and Ferricyanides, in Encyclopedia of Chemical Technology, R. G. Kirk and D. F. Othmer (eds.), N. Y., Interscience Encyclopedia, 4 (1949) 726.
16. T. ICHIDA, R. SHINJO, Y. BANDE and T. TAKADA, J. Phys. Soc. Japan, 29 (1970) 1109.
17. W. KERLER, W. NEUWIRTH, E. FLUCK, P. KUHN and S. ZIMMERMANN, Z. Physik, 173 (1963) 321.
18. W. MEISEL and G. KREYSA, Z. Anorg. Allgem. Chem., 395 (1973) 31.
19. "Zapp", Vulcan Material Plástico S. A., Rio de Janeiro, Brasil.

RÉSUMÉ — Le ferrocyanure de potassium trihydraté, $K_4Fe(CN)_6 \cdot 3H_2O$, a été chauffé en présence d'oxygêne dans un Derivatograph, dans des conditions bien déterminées de masse et de vitesse de chauffage. Le chauffage a été interrompu à diverses températures et les spectres Mössbauer ainsi que les diffractogrammes de rayons X ont été enregistrés aprês trempe du matériau à la température ambiante. On a étudié de cette façon le déroulement de la réaction; on décrit les avantages et les inconvénients de chacune de ces techniques. On a pu déceler la présence de $K_4Fe(CN)_6$, α-Fe_2O_3, Fe_3O_4 Fe_3C, Fe, FeO, $KFeO_2$, β-FeOOH, KOCN, K_2CO_3 et KCN aux différentes étapes du traitement thermique.

ZUSAMMENFASSUNG — Kaliumhexacyanoferrat(II)trihydrat, $K_4[Fe(CN)_6.3H_2O$ wurde unter kontrollierten Bedingungen in einem Derivatographen in Gegenwart von Sauerstoff erhitzt. Das Aufheizen wurde bei verschiedenen Temperaturen gestoppt und Mössbauer-Spektren, sowie Röntgendiffraktogramme aufgenommen. Der Reaktionsweg wurde auf diese Weise untersucht und die Vor- und Nachteile jeder der Techniken beschrieben. Bei den verschiedenen Stufen des thermischen Vorganges konnten $K_4[Fe(CN)_6]$, α-Fe_2O_3, Fe_3O_4, Fe_3C, Fe, FeO, $KFeO_2$, β-FeOOH, KOCN, K_2CO_3 und KCN nachgewiesen werden.

Резюме — Тригидрат гексациано-железо (II)-кислый калий — $K_4Fe/CИ)_6 . 3H_2O$-был нагрет в дериватографе в присутствии кислорода при контролируемой массе и скорости. Нагревание прекращалось при различных температурах и измерялись мессбауэровские спектры и рентгеновские диффрактограммы охлажденного до комнатной температуры материала. Таким образом было изучено протекание реакций и описаны преимущества и недостатки каждого из этих методов. Было возможным показать на различных стадиях термического процесса присутствие $K_4Fe(CN)_6$, α-Fe_2O_3, Fe_3O_4, Fe_3C, Fe, FeO, $KFeO_2$, β-FeOOH, KOCN, K_2CO_3 и KCN.